

Determination of $\text{UO}_2(\text{s})$ dissolution rates in a hydrogen peroxide medium as a function of pressure and temperature

Ignasi Casas^a, Maria Borrell^a, Laia Sánchez^a, Joan de Pablo^{a,b},
Javier Giménez^{a,*}, Frederic Clarens^b

^a *Departament d'Enginyeria Química H4, Universitat Politècnica de Catalunya (UPC), Avda. Diagonal 647, 08028 Barcelona, Spain*

^b *CTM Centre Tecnològic, Avda. Bases de Manresa, 1, 08240 Manresa, Spain*

Received 30 March 2007; accepted 28 August 2007

Abstract

A continuously stirred flow-through tank reactor has been developed and successfully used to determine rates of dissolution of powdered samples of uranium dioxide at pressure and temperature conditions above the ambient values. The experiments have been performed in a temperature range from 20 to 50 °C and a total hydraulic pressure ranging from 1 to 32 bar. Experiments have been performed in a test solution containing 10^{-4} mol/L of H_2O_2 , 3×10^{-3} mol/L of NaHCO_3 and, finally, NaClO_4 to get a constant ionic strength of 0.1 mol/L. An empirical equation has been obtained that describes the results in the experimental range studied and gives a good concordance with values obtained at ambient conditions in other works. On the other hand, scanning electron microscopy (SEM) has shown that the solid surface has homogeneously reacted, and, in addition, no secondary solid phase has been formed on the UO_2 surface.

© 2008 Elsevier B.V. All rights reserved.

PACS: 82.55; 28.41.T; 28.41.K; 82.50.G

1. Introduction

High level nuclear wastes are one of the most hazardous materials produced at present by human activities. The main component of such wastes is uranium (IV) dioxide (approx. 95–98% of the total wastes). The study of the future evolution of these materials is critical to assess the performance of the waste management and to prevent the possibilities of future impacts to the biosphere [1,2].

One of the solutions proposed at present to deal with these wastes is to bury them in deep geological repositories, where the low solubility of uranium dioxide will constitute one of the main barriers to prevent the mobilization of the radionuclides contained in the nuclear wastes. However, it must be taken into account the possibility of oxidation of

uranium to its sixth oxidation state, which drastically increases the solubility of the waste matrix as well as the release of the radionuclides that contain [3,4]. Several oxidizing agents can be responsible for the transition from UO_2 to UO_{2+x} . Most likely, they will be formed by the radiolysis of water due to the radiation emitted by the wastes and once they get in contact with groundwater. Among the different species formed by this radiolytic process, hydrogen peroxide is one of the main molecular oxidants produced [5–7], actually, according to Ekeroth et al. [23], hydrogen peroxide is the only oxidant of significance in spent nuclear fuel dissolution.

In previous works [8,9], we have studied the effect of this oxidising agent on UO_2 in order to develop an oxidation/dissolution mechanism under chemical conditions relatively close to the ones expected in a deep geological repository. However, the effect of parameters such as temperature (due to the heat emitted by the wastes) and pressure (due to the depth of the repository), which might have a

* Corresponding author. Tel.: +34 934017388; fax: +34 934015814.
E-mail address: francisco.javier.gimenez@upc.edu (J. Giménez).

significant effect in the whole mechanism, have not been simultaneously studied in detail, yet. Actually, there are no data in literature related to the effect of pressure.

In the present work we have developed and used a continuously stirred flow-through tank reactor to determine the kinetics of dissolution of UO_2 in the presence of H_2O_2 and as a function of hydrostatic pressure and temperature. In the output flow we measured both uranium and hydrogen peroxide concentrations until the system reached a steady-state condition. At that point, we used the uranium concentrations, the flow rate and the total area of solid inside the reactor to calculate the rates of UO_2 dissolution ($\text{mol m}^{-2} \text{s}^{-1}$).

2. Experimental

2.1. Reactor design

The reactor was built in an A240 (ASTM) iron steel, based on its corrosion, mechanical and thermal characteristics considering the experimental conditions proposed. Its total inner volume was 100 mL.

The reactor was designed to hold a maximum working pressure of 100 bar and a maximum temperature of 100 °C, both of them far above the conditions to be used in the experiments.

The inflow solution entered to the bottom of the reactor while the exit was located in the top of the semi spherical shaped cover. In this way we ensure a good contact between the test solution and the solid sample while, at the same time, we prevent the formation of a gas chamber inside of the reactor. A Teflon magnetic stirrer bar together with four deflectors located inside the reactor ensured a good solution mixing, to avoid concentration gradients throughout the volume as well as to ensure, again, a good contact between the solid sample and the test solution.

The solid was located in a plate to keep it away from the stirrer to prevent in this way the possibility of mechanical impact on the solid phase.

2.2. Experimental setup

The test solution was pumped by using a high performance chromatography pump that allowed the high pressures to be used. A pressure regulator was used to adjust the value to the preset one, which was indicated by a pressure sensor. A security valve was included to avoid any accidental increase of the pressure above the value for which the reactor had been designed. The system was checked to a maximum pressure of 70 bar without problems. This value is far above the values that were expected to be used in the experiments. Finally, a by-pass valve allowed working at ambient pressure. In Fig. 1 we present a scheme of the pressure setting system.

To keep the temperature to the desired values, we submerged the reactor inside a thermostatic bath with a temperature control.

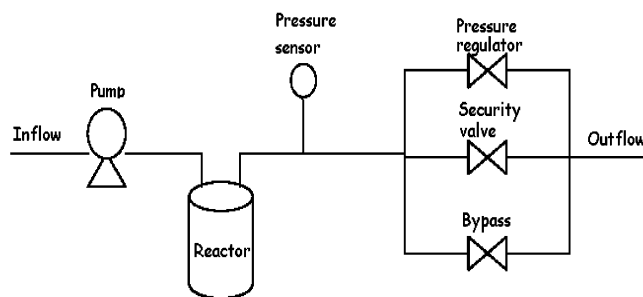


Fig. 1. Scheme of the experimental setup used to set the desired pressure.

Samples of the outflow solution were automatically collected at preset times by using a Gilson® sample collector.

2.3. Experimental conditions

A weight of 1022 g of $\text{UO}_2(\text{s})$ was introduced in the sample holder. The solid had been previously crushed and sieved. In the experiments we used the fraction with a mean particle size ranging from 100 to 300 μm . The specific surface area of this fraction was determined by the BET method to be $0.009 \pm 0.001 \text{ m}^2/\text{g}$.

The inflow test solution contained 10^{-4} mol/L of H_2O_2 , $3 \times 10^{-3} \text{ mol/L}$ of NaHCO_3 and 0.097 mol/L of NaClO_4 to give a total ionic strength of 0.1 mol/L. The test solution was pumped at a flow rate of 0.6 mL/min. However, this parameter was determined at each sampling point by weight to account for possible fluctuations.

The temperature of the experiments ranged from 20 to 50 °C, while the pressure ranged from 1 to 32 bar. A total of eight different experiments were performed and their characteristics are summarized in Table 1. For each experiment, known volumes of the outflow solution were sampled and in each case both uranium and hydrogen peroxide concentrations were determined by ICP-MS and a Chemiluminescence method (CL-1, Camspec) [10,11], respectively. Each experiment was continued until we ensured the attainment of a steady-state condition. At that point, from the uranium concentration, the flow rate and the total surface area of the solid we determined the dissolution rate as

$$r = [\text{U}]_{\text{ss}} \cdot Q/A, \quad (1)$$

Table 1
Summary of the experimental conditions of the eight runs performed

Exp. code	Pressure		Temperature	
	(Pa)	(bar)	(°C)	(K)
U 1-293	1×10^5	1	20	293
U 6-293	6×10^5	6	20	293
U 16-293	16×10^5	16	20	293
U 32-293	32×10^5	32	20	293
U 32-303	32×10^5	32	30	303
U 32-323	32×10^5	32	50	323
U 1-303	1×10^5	1	30	303
U 1-323	1×10^5	1	50	323

where r in $\text{mol m}^{-2} \text{s}^{-1}$, is the dissolution rate, $[U]_{\text{ss}}$, in mol/L , is the uranium concentration in solution at the steady-state, Q in L/s , is the flow rate, and A in m^2 , is the total surface area of the solid.

3. Results and discussion

In Fig. 2, some examples of the uranium concentrations measured in the outflow solution are presented. It can be seen in the figure the effect on the uranium concentration of changing the experimental conditions, either the temperature or the total pressure. In all cases, a final steady-state is achieved, from which we calculated the rates of dissolution by using Eq. (1). It can be observed that this steady-state situation takes a longer time in the first run, which is most likely due to the initial dissolution of fines or initially present oxidised phases on the UO_2 surface.

In Table 2 we summarize the results obtained for the eight series of experiments performed. In addition to the steady-state uranium concentrations and the rates of dissolution, we also present in this table the hydrogen peroxide concentrations measured on the outflow solution once the uranium steady-state concentration was reached.

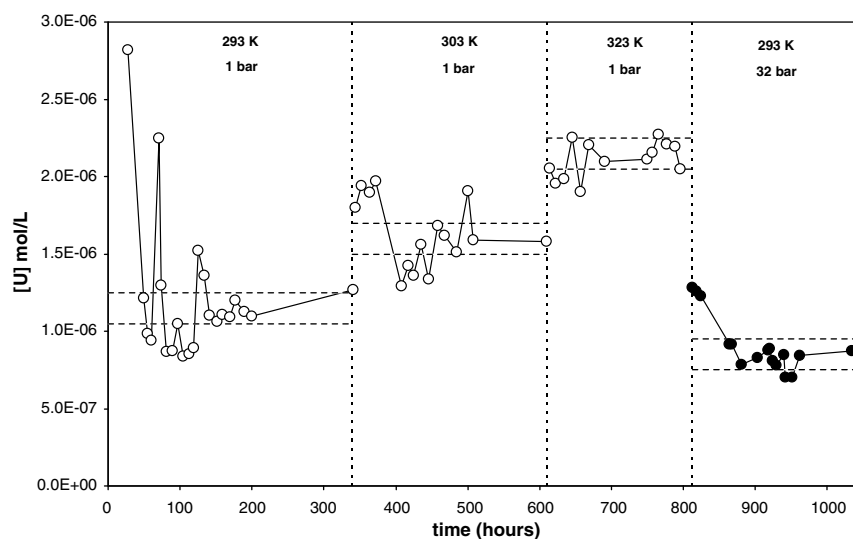


Fig. 2. Uranium concentrations measured in the outflow solution for some of the runs performed. Horizontal dashed lines show the interval of concentrations considered as steady-state and used to calculate the rates of dissolution. Vertical dashed lines show where the experimental conditions were changed.

Table 2
Hydrogen peroxide and uranium steady-state concentrations measured in the outflow solution

Exp. code	Outflow $[\text{H}_2\text{O}_2]_{\text{ss}}$ (mol/L)	Outflow $[U]_{\text{ss}}$ (mol/L)	r ($\text{mol m}^{-2} \text{s}^{-1}$)
U 1-293	5.57×10^{-5}	$1.1 \times 10^{-6} \pm 2 \times 10^{-7}$	$1.1 \times 10^{-9} \pm 1 \times 10^{-10}$
U 6-293	7.24×10^{-5}	$2.1 \times 10^{-6} \pm 3 \times 10^{-7}$	$2.1 \times 10^{-9} \pm 3 \times 10^{-10}$
U 16-293	8.12×10^{-5}	$1.6 \times 10^{-6} \pm 2 \times 10^{-7}$	$1.6 \times 10^{-9} \pm 3 \times 10^{-10}$
U 32-293	2.41×10^{-5}	$8.1 \times 10^{-7} \pm 6 \times 10^{-8}$	$1.0 \times 10^{-9} \pm 1 \times 10^{-10}$
U 32-303	2.50×10^{-5}	$2.0 \times 10^{-6} \pm 2 \times 10^{-7}$	$2.3 \times 10^{-9} \pm 4 \times 10^{-10}$
U 32-323	1.25×10^{-5}	$2.9 \times 10^{-6} \pm 2 \times 10^{-7}$	$3.1 \times 10^{-9} \pm 3 \times 10^{-10}$
U 1-303	5.86×10^{-5}	$1.5 \times 10^{-6} \pm 2 \times 10^{-7}$	$1.8 \times 10^{-9} \pm 2 \times 10^{-10}$
U 1-323	1.73×10^{-5}	$2.1 \times 10^{-6} \pm 1 \times 10^{-7}$	$2.4 \times 10^{-9} \pm 3 \times 10^{-10}$

The rates of dissolution are calculated from the experimental values and using Eq. (1).

Fig. 3 shows a sequence of SEM pictures of the UO_2 taken at the beginning and at the end of the experiments, respectively. From these pictures we deduced, first, that a homogeneous reaction did take place on the solid surface, implying a good solid/solution contact inside the reactor. Second, it was evident the preferential attack on the grain boundaries, which were clearly open at the end of the experimental runs, though, also some attack was evident on the grain surfaces, showing the aggressive reaction due to the hydrogen peroxide. And, third, it was not possible to find any indication of a secondary phase formation, as it is assumed with this experimental device, and which indicates that the results obtained are really representative of the dissolution of UO_2 .

3.1. Effect of temperature on the $\text{UO}_2(s)$ dissolution rate

The effect of temperature on the rate of dissolution might be basically described by using the Arrhenius equation:

$$\ln k = \ln A - (E_a/R) \cdot (1/T), \quad (2)$$

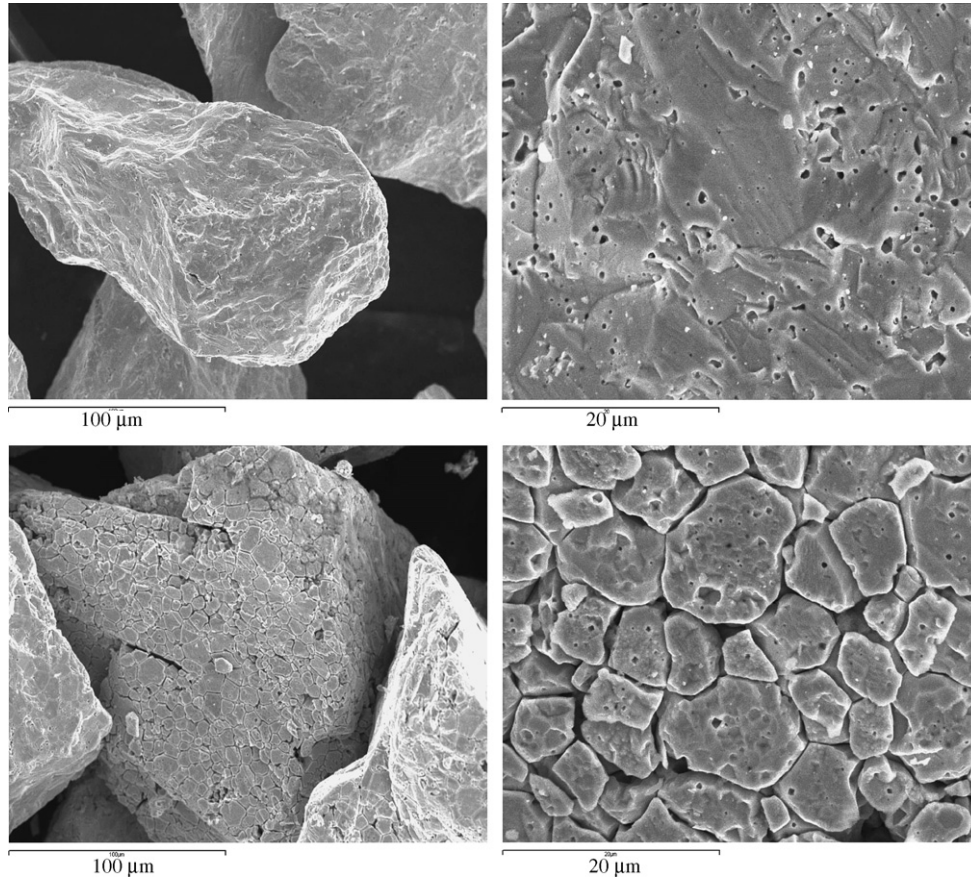


Fig. 3. SEM pictures of the $\text{UO}_2(\text{s})$ sample at different magnifications. The images were taken before (two upper pictures) and after (two lower pictures) the experimental runs.

where k is the rate dissolution constant, E_a is the activation energy, A is the pre-exponential factor, R is the gas constant and T stands for the temperature.

If the logarithm of the rate of dissolution (r), directly proportional to k , is plotted against the reciprocal of the temperature, the slope of the fitting to the experimental data allows to determine the activation energy of the dissolution reaction and from this value some observations of the rate controlling step can be deduced [12,13].

3.2. Effect of pressure on the $\text{UO}_2(\text{s})$ dissolution rate

The effect of this parameter on the dissolution rate constant has been studied by using the equation described by Brezonik [14]

$$\ln \frac{k_P}{k_{P_0}} = \frac{-\Delta V^\ddagger \cdot (P - P_0)}{R \cdot T}, \quad (3)$$

where k_P and k_{P_0} are the kinetic constants, P and P_0 are the pressure and initial pressure (in bar), respectively, and T is the temperature (in K). In this equation, ΔV^\ddagger stands for the activation volume, that is, the difference between the molar volume of the species in the transition state and the molar volume of the reactant products. In the experimental pressure range of the present work we assumed (based on con-

siderations given in [14]) that this term is independent on the pressure. This approximation allows us to plot the experimental $\log r$ values versus the term $(P - 1)/T$ and from the resulting figure it might be possible to deduce the dependence of the dissolution rate on the hydrostatic pressure.

3.3. Effect of $[\text{H}_2\text{O}_2]$ on the $\text{UO}_2(\text{s})$ dissolution rate

As in previous studies [8,9,15] UO_2 dissolution rate has been found to be directly proportional to the hydrogen peroxide concentration, the reaction being first order with respect to H_2O_2 .

3.4. Multivariate semi-empirical rate equation

The different effects briefly described in the preceding paragraphs show some inter dependency, which makes unreasonable to perform the study of their effects on the rate of dissolution of UO_2 independently one from each other.

For that reason, we performed a multivariate analysis of the data, taken in this way into consideration all the experimental variables at the same time.

The equation that we used to fit to the data, included the different dependencies presented in the preceding sections

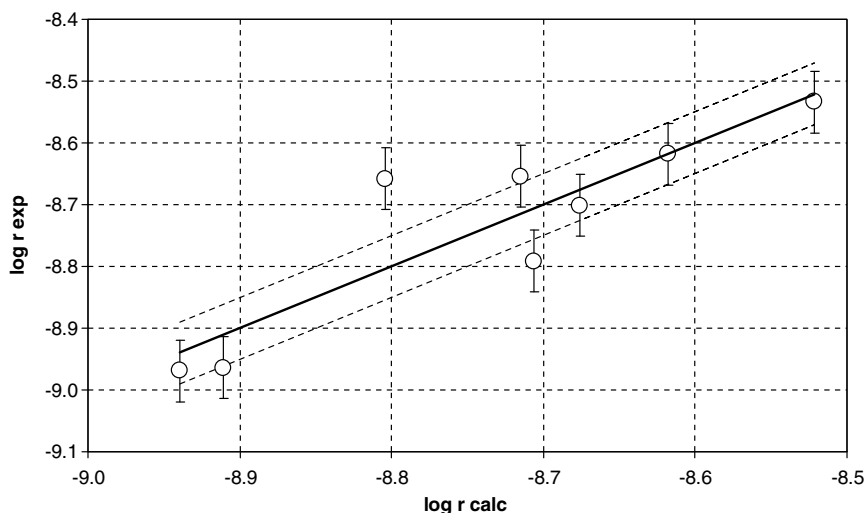


Fig. 4. Experimentally determined rates of dissolution in front of the rates of dissolution calculated by using Eq. (5) in the text. Solid line shows the linear regression, which corresponds to the equation $y = x$, while dashed lines give the 95% confidence intervals.

on temperature, pressure and hydrogen peroxide concentration. The resulting semi-empirical equation to be used is as follows:

$$\log r = k + n_1 \cdot ((P - 1)/T) + n_2 \cdot (1/T) + n_3 \cdot \log [\text{H}_2\text{O}_2]. \quad (4)$$

The fitting of this equation to the experimental dissolution rates determined in this work allowed the determination of the different fitting parameters k , n_1 , n_2 and n_3 , and the final equation became as follows:

$$\log r = 1(\pm 3) + 2(\pm 1) \cdot ((P - 1)/T) - 2077(\pm 600) \cdot (1/T) + 0.7(\pm 0.3) \cdot \log [\text{H}_2\text{O}_2] \quad (r^2 = 0.80). \quad (5)$$

Fig. 4 is a plot of the experimentally determined dissolution rates versus the calculated values obtained by using Eq. (5). The solid line gives the linear dependency of the two sets of values ($y = x$), while the dashed lines indicate (based on the statistical analysis of the fitting) the intervals for the 95% of confidence. As it can be seen, a rather good concordance is obtained.

By studying the resulting semi-empirical equation some conclusions can be drawn.

The fitting equation implies that pressure has some effect on the dissolution rate, though, the dependency is found not to be very important in the experimental range studied. As a comparison, we found that using oxygen as oxidant, the dissolution of UO_2 was found to be independent of pressure up to 10 bar [16,17].

Considering the temperature dependency term, the activation energy value for the dissolution reaction can be calculated

$$E_a = 40 \pm 11 \text{ kJ/mol.}$$

According to [12], values of E_a lower than 40 kJ/mol suggest that the dissolution rate is controlled by diffusion while higher values suggest a surface dissolution reaction controlled rate. In our case we found a value which is very close to the transition value proposed, which makes very difficult to ascertain whether we should account preferentially for a diffusion or a surface dissolution control for the dissolution reaction.

Anyway, the E_a value determined in this work is in fairly good agreement with activation energy values for the overall oxidative dissolution process obtained by other researchers either for spent nuclear fuel [18], UO_2 [19] and uraninite [20], with values typically ranging from 20 to 60 kJ/mol. It is also similar to the value obtained by de Pablo et al. [21] for the elementary process of HCO_3^- coordination on the U(VI) sites at the solid surface.

Finally, with respect to the dependency on the hydrogen peroxide concentration, a comparison can be made with some experimental data [22] obtained by using a continuous flow-through system and the following experimental conditions:

$$[\text{HCO}_3^-] = 3 \times 10^{-3} \text{ M}; \quad [\text{H}_2\text{O}_2] = 10^{-4} \text{ M}; \\ P = 1 \text{ atm and } T = 293 \text{ K.}$$

They obtained a $\log r$ value of -8.52 , while using Eq. (5) a value of -8.59 is obtained. Taking into account this good concordance, it seems clear that Eq. (5) gives a good representation of experimental published values and it could be used to determine rates of dissolution under conditions closer than the ones than can be found either in natural uraninite deposits or in engineered nuclear waste deposits.

4. Conclusions

A continuously stirred flow-through tank reactor has been developed to determine rates of dissolution of

powdered samples of UO_2 at temperature and pressure conditions above the ambient values (20–50 °C and 1–32 bar, respectively).

A multivariate analysis of the experimental dissolution rates obtained has been performed and the results have been fitted with the following semi-empirical equation:

$$\log r = 1(\pm 3) + 2(\pm 1) \cdot ((P - 1)/T) - 2077(\pm 600) \cdot (1/T) + 0.7(\pm 0.3) \cdot \log [\text{H}_2\text{O}_2].$$

Acknowledgments

This work was financially supported by ENRESA (Spanish Radioactive Waste Management Co), and the European Commission.

References

- [1] J. Bruno, R.C. Ewing, *Elements 2* (2006) 343.
- [2] L.H. Johnson, D.W. Shoesmith, in: W. Lutze, R.C. Ewing (Eds.), *Radioactive Waste Forms for the Future*, Elsevier, New York, 1988, p. 635.
- [3] I. Casas, J. de Pablo, J. Giménez, M.E. Torrero, J. Bruno, E. Cera, R.J. Finch, R.C. Ewing, *Geochim et Cosmochim. Acta* 62 (1998) 2223.
- [4] J. Bruno, I. Casas, I. Puigdomènech, *Geochim et Cosmochim. Acta* 55 (1991) 647.
- [5] B. Grambow, A. Loida, P. Dressler, H. Geckeis, J. Gago, I. Casas, J. de Pablo, J. Giménez, M.E. Torrero, Chemical reaction of fabricated and high burnup spent UO_2 fuel with saline brines. European Commission, Final Report EUR-17111, 1997.
- [6] T.E. Eriksen, U.-B. Eklund, L. Werme, J. Bruno, *J. Nucl. Mater.* 227 (1995) 76.
- [7] K.-A. Hugues Kubatko, K.B. Helean, A. Navrotsky, P.C. Burns, *Science* 302 (2003) 1191.
- [8] J. de Pablo, I. Casas, F. Clarens, F. El Aamrani, M. Rovira, *Mater. Res. Soc. Symp. Proc.* 663 (2001) 409.
- [9] F. Clarens, J. de Pablo, I. Casas, J. Giménez, M. Rovira, J. Merino, E. Cera, J. Bruno, J. Quiñones, A. Martínez-Esparza, *J. Nucl. Mater.* 345 (2005) 225.
- [10] D. Price, P.J. Worsfold, F.C. Montoura, *Anal. Chim. Acta* 298 (1994) 121.
- [11] F. Clarens, J. Giménez, J. de Pablo, I. Casas, M. Rovira, J. Dies, J. Quiñones, A. Martínez-Esparza, *Radiochim. Acta* 93 (2005) 533.
- [12] A.C. Lasaga, *J. Geophys. Res.* 89 (1984) 4009.
- [13] A.C. Lasaga, J.M. Soler, J. Ganor, T.E. Burch, K.L. Nagy, *Geochim. et Cosmochim. Acta* 58 (1994) 2361.
- [14] P.L. Brezonik, *Chemical Kinetics & Process Dynamics in Aquatic Systems*, Lewis Publishers, USA, 1994.
- [15] J. Giménez, E. Baraj, M.E. Torrero, I. Casas, J. de Pablo, *J. Nucl. Mater.* 238 (1996) 64.
- [16] J.B. Hiskey, *Trans. Inst. Min. Metall. (Sect. C: Mineral Processes Extr. Metall.)* 89 (1980) 145.
- [17] W.E. Schortmann, M.A. DeSea, in: *Second United Nations International Conference on the Peaceful Uses of Atomic Energy Proceedings*, vol. 3, 1958, p. 333.
- [18] W.J. Gray, H.R. Leider, S.A. Steward, *J. Nucl. Mater.* 190 (1992) 46.
- [19] S. Aronson, R.B. Roof Jr., J. Belle, *J. Chem. Phys.* 27 (1957) 137.
- [20] D.E. Grandstaff, *Econ. Geol.* 8 (1976) 1493.
- [21] J. de Pablo, I. Casas, J. Giménez, M. Molera, M. Rovira, L. Duro, J. Bruno, *Geochim. et Cosmochim. Acta* 63 (1999) 3097.
- [22] F. Clarens, PhD Thesis 'Efecto de la radiólisis y de los productos radiolíticos en la disolución del UO_2 : Aplicación al modelo de alteración de la matriz del combustible nuclear gastado', Barcelona, Spain, 2004.
- [23] E. Ekeröth, O. Roth, M. Jonsson, *J. Nucl. Mater.* 355 (2006) 38.